THE JOURNAL OF PHYSICAL CHEMISTRY A

ARTICLE

pubs.acs.org/JPCA

Filament-Driven Impulsive Raman Spectroscopy

Johanan H. Odhner, Erin T. McCole, and Robert J. Levis*

Department of Chemistry and Center for Advanced Photonics Research, Temple University, Philadelphia, Pennsylvania 19122, United States

ABSTRACT: Vibrational Raman spectroscopy is performed in the gas phase using a femtosecond laser pulse undergoing filamentation as an impulsive excitation source. The molecular coherence induced by the filamentary pulse is subsequently probed using a narrowband, sub-picosecond laser pulse to produce Raman spectra of gas phase species in a few tens of milliseconds (~10 laser shots). Pulse shortening with concomitant spectral broadening during filamentation results in a pulse that is both sufficiently short and of sufficient spectral power density to impulsively excite the highest energy ground state vibrations (up to 4158 cm^{-1} corresponding to H_2). Gas phase detection of chloroform, methylene chloride, cyclohexane, toluene, pentane, triethylamine, ammonia, nitromethane, and gasoline is performed.

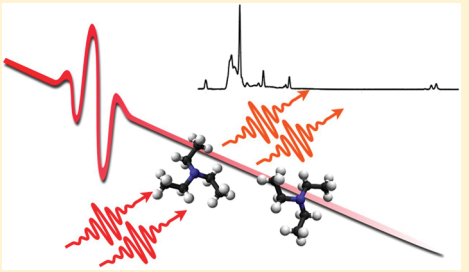

INTRODUCTION

Stand-off detection of gas phase molecules using Raman spectroscopy is challenging. The low scattering cross-section (on the order of $\sim 10^{-30}$ cm^2), the low density of molecules in the gas phase (10^{19} cm^{-3}, in comparison with the solid or liquid state density of 10^{22} cm^{-3}), and the isotropic spatial distribution of the Raman-scattered light make spontaneous Raman spectroscopy difficult to perform under atmospheric pressure conditions. Coherent, nonlinear laser spectroscopy can increase the scattering efficiency up to 5 orders of magnitude, because the signal scales as the square of the number of coherent oscillators in a sample rather than linearly, as is the case for an ensemble of incoherent oscillators. In addition, the coherent Raman signal occurs in a directed beam, allowing for higher signal collection efficiencies. Previous studies of coherent Raman spectroscopy in the condensed phase using coherent Raman spectroscopy (c.f., refs 1−5) have paved the way for gas-phase stand-off Raman spectroscopy.

Significant strides have been made toward stand-off detection using coherent Raman spectroscopy,[6−9] but diffraction in the transverse plane limits the maximum intensity that a "weak" (i.e., linearly propagating) laser beam can achieve at a given distance. Additionally, tunable narrowband or extremely broadband pulses are necessary for detection over a wide vibrational window, requiring experimental components such as optical parametric amplifiers (OPA) or hollow-core fibers (HCF) to generate the necessary tunability or bandwidth. A means for chirp precompensation is also required in the latter example to produce a temporally short pulse at the target location. The efficiency of OPA and HCF systems also results in a pulse with significantly less energy than the input, further reducing the maximum intensity at the detection point for long distances. In this work, we introduce a method that circumvents the problem of geometric focusing, as well as the complications arising in the generation of the sufficiently broad spectral bandwidth necessary for detection of the entire vibrational spectrum.

Filament-driven impulsive Raman spectroscopy makes use of the intrinsic pulse shortening that occurs during filamentation to impulsively excite the entire vibrational spectrum of the propagation medium. Impulsive stimulated Raman scattering (ISRS) employs a laser pulse shorter than the vibrational period(s) of the molecule(s) under interrogation ($\tau_{laser} < \tau_{vib}$) to create a time-dependent change in the polarizability of the sample that oscillates at the vibrational frequency, $1/\tau_{vib}$.[10] In principle, ISRS can be used to measure the entire Raman spectrum of arbitrarily complex molecules in a single laser shot. The essential requirement for the pump pulse is that its duration must be shorter than the vibrational period of the highest energy vibrational mode present in the molecule. For the purpose of molecular detection and identification, the "entire" Raman spectrum constitutes the ground-electronic state vibrational spectrum (between 0 and ~4000 cm^{-1}). We note that the corresponding maximum pulse duration spanning 4000 cm^{-1} of bandwidth (base-to-base) is roughly 8.3 fs, a pulse duration which still requires considerable effort to generate with conventional methods (i.e., OPA or HCF). After excitation of the medium by the pump pulse, a second, time-delayed laser pulse (ω_{probe}) traversing the coherently excited medium will interfere to produce sidebands at the Stokes ($\omega_{probe} - \omega_{vib}$) and anti-Stokes ($\omega_{probe} + \omega_{vib}$) frequencies if the pulse is long compared with the vibrational period ($\tau_{probe} \gg \tau_{vib}$) and the time-delay between the pump and probe pulses, t, is shorter than the dephasing time of the vibration. Impulsive excitation requires only that the pump pulse contain *features* shorter than the vibrational period that do not destructively interfere over the total duration of the pulse.[11]

The spectroscopic method implemented here utilizes the inherent pulse shortening that occurs during the filamentation of a femtosecond pulse in air to form the impulsive Raman pump.

Received: July 29, 2011
Revised: September 28, 2011
Published: October 07, 2011

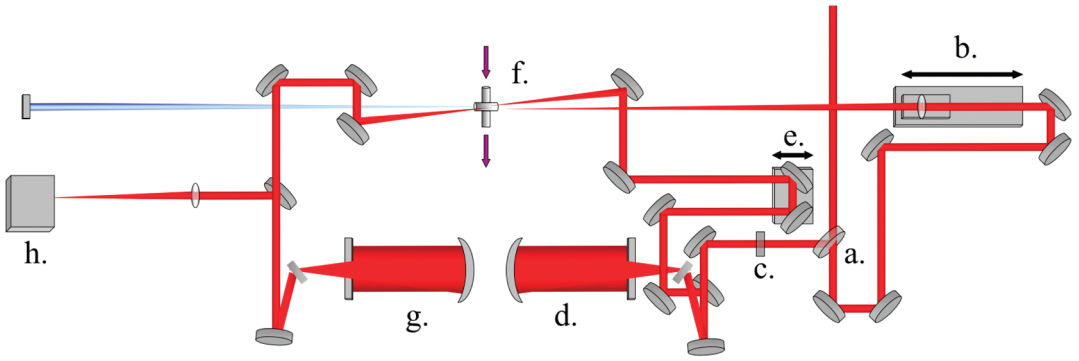

Figure 1. Experimental setup for filament-based Raman spectroscopy. (a) beamsplitter, (b) 2-m lens and 30-cm stage, (c) half-wave plate, (d) 4-f spectral filter, (e) delay stage, (f) sample, (g) 4-f Rayleigh line filter, and (h) spectrometer.

Filamentation occurs when a laser pulse propagates through a medium with a peak power higher than the threshold (critical) power for self-focusing in the medium, $P_{crit} = 3.77\lambda^2/8\pi n_0 n_2$,[12] where λ is the carrier wavelength, and n_0 and n_2 are the index of refraction and intensity-dependent index of refraction of the medium, respectively. In this case, the nonlinear focusing of the pulse leads to a regime of high-intensity propagation (10^{13} Wcm^{-2}),[13] where competition between self-focusing and dispersive effects in the medium (such as plasma generation, diffraction, and higher-order nonlinearities) takes place.[14] This, in turn, leads to the radial confinement of the laser beam well beyond the Rayleigh range of the focused laser beam that is anticipated from linear optics.[15] Under such conditions, substantial reshaping of the temporal, spatial, and spectral properties of the pulse occurs (c.f., refs 16 and 17). These effects contribute to pulse shortening to durations of a few femtoseconds.[18,19] The high energy density in a filament and the pulse shortening are particularly advantageous when considering the application of coherent Raman spectroscopy to stand-off detection scenarios. Recently, filamentation has been used for time-resolved vibrational Raman spectroscopy of several pure molecular gases.[20−22] Calegari, et al. used filamentation in an argon gas cell to produce a white-light continuum that was subsequently compressed to 10 fs with chirped mirrors and used for ISRS in a second gas cell. The observation of the hydrogen vibration at ∼4155 cm^{-1} (τ_{vib}∼8 fs) revealed the occurrence of pulse shortening in the second cell, facilitating vibrational excitation. Here we expand on our previous work using relatively long (∼50 fs) driving pulses self-shortened in air[22,23] coupled with narrowband (∼25 cm^{-1}) detection to demonstrate utility of filament-driven gas phase Raman spectroscopy in several organic solvents, an inorganic solvent, and fuels.

EXPERIMENTAL SECTION

The experimental setup is shown in Figure 1. Laser pulses were generated in a Ti:sapphire-based chirped pulse amplifier system producing 2.5 mJ, 45 fs pulses at a 1 kHz repetition rate. The pulse was split into pump (2 mJ) and probe (0.5 mJ) beams. The intense pump pulse was loosely focused into atmospheric air using a 2-m lens, generating a visible filamentation column extending over ∼65 cm and having two focusing cycles. The filament was optimized for maximum spectral broadening by an aperture (before the 2-m lens) and by changing the chirp of the laser pulse in the amplifier compressor. After filamentation, the pump spectrum was broadened from a bandwidth of 800 cm^{-1} at 800 nm (base-to-base) to a bandwidth of >20 000 cm^{-1} with colors extending from 330 to 920 nm.

Spectral filtering in the Fourier plane of a zero-dispersion, folded 4-f stretcher comprised of a grating, cylindrical mirror, and slit generated the longer duration probe pulse. The probe pulse polarization was then rotated and the beam was focused using a 0.5-m lens into the filament channel at a small angle (<1.3°) with respect to the filament axis. The slit width in the filter was variable with a typical spectral width of 23 cm^{-1}, corresponding to a Fourier transform-limited pulse duration of 640 fs. The probe pulse energy was 12 ± 2 μJ under these conditions.

The temporal delay between the pump and probe beams was controlled by a delay stage in the probe beam path and the spatial overlap between the filament and the probe beams was controlled by adjusting the transverse and longitudinal positions of the 2-m lens. The 2-m lens was mounted on a 30-cm long translation stage and could be moved on the table to provide a total translation range of 100 cm. The pump−probe time delay was fixed at +770 fs (pump preceding probe) to minimize cross-phase modulation between the probe beam and the intense pump while maximizing the signal from the impulsively excited molecular coherence. The optimum position in the laser filament (the distance from the 2-m lens) for Raman spectroscopy was determined by maximizing the intensity of the ambient water O−H vibrational stretching mode at 3657.1 cm^{-1}, which is the highest energy vibration observed under ambient conditions. The highest signal intensity for this mode was observed ∼250 cm from the 2-m lens. The fact that the highest signal intensity was measured 50 cm after the geometric focus of the lens is attributed to the nonlinear propagation of the pump pulse during filamentation. After the pump−probe overlap in the sample, the probe pulse was filtered using a second 4-f filter to remove the fundamental probe wavelength then focused into a spectrometer (USB4000, Ocean Optics). Note that a small blue-shifted spectrometer artifact was created for each feature in the spectrum (for example at 2420 cm^{-1} in Figure 2 for the nitrogen line at 2342 cm^{-1}). This effect is most notably detected in conjunction with peaks close to the saturation level of the CCD array. Spatially filtering a given "real" Raman feature in the Fourier plane of the second 4-f filter with a razor blade removed the artifact from the spectrum, confirming that it originates in the spectrometer rather than from the Raman response of the sample. Both CSRS and CARS signals were observable in our experiments, but only the anti-Stokes spectrum is considered here.

Vapor phase samples were prepared by passing an inert gas (argon) through a flask of the liquid sample to be measured.

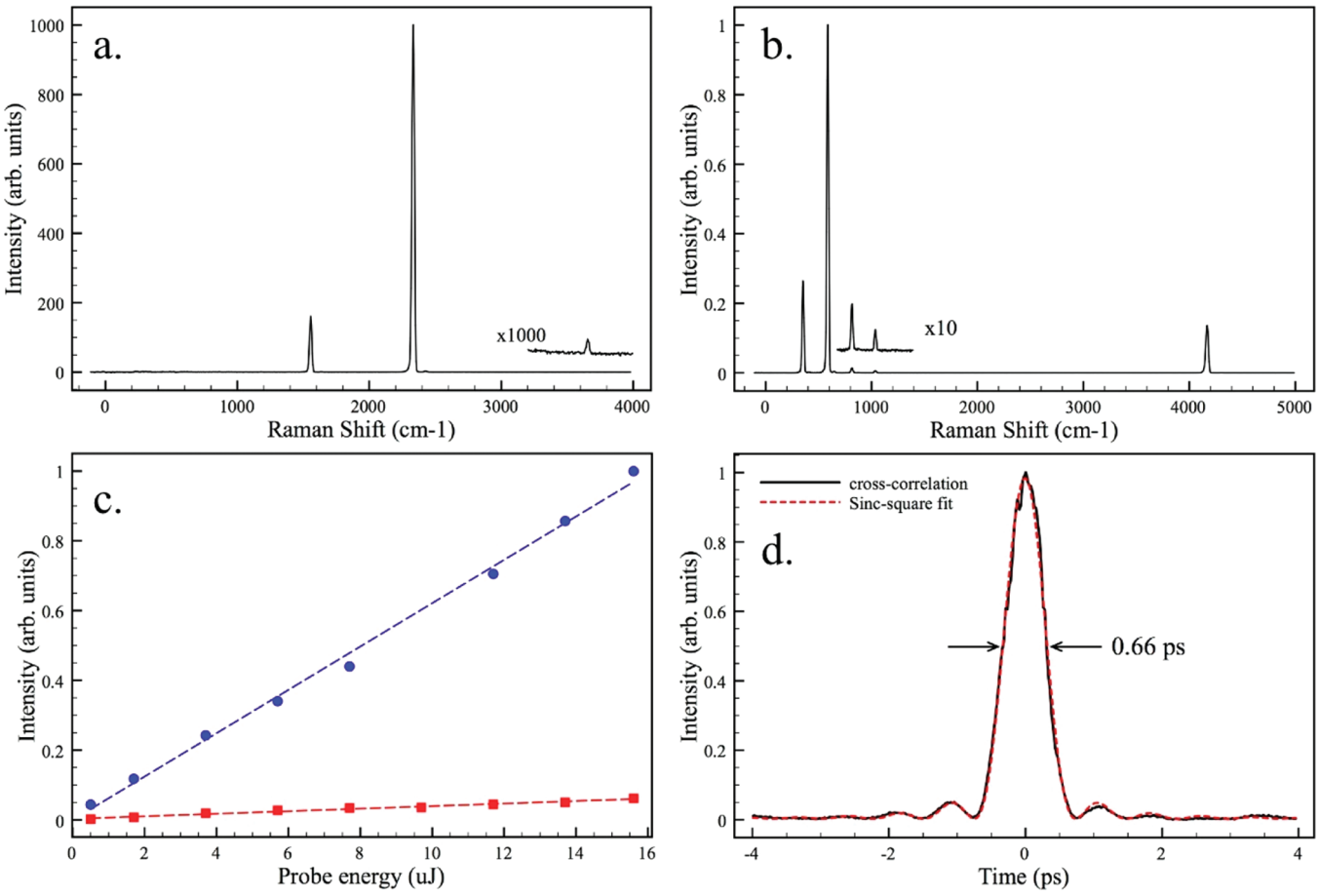

Figure 2. The Raman spectra of (a) air and (b) hydrogen demonstrate the utility of filament-assisted impulsive Raman spectroscopy. The peaks at 1558.7, 2333.3, and 3656 cm^{-1} in (a) correspond to the oxygen, nitrogen, and water Raman lines, respectively. The water line was measured separately from oxygen and nitrogen without neutral density filters. The signals at 354.3, 586.7, 813.6, and 1034 cm^{-1} in (b) correspond to the rotational Raman lines of hydrogen and the signal at 4155 cm^{-1} is the hydrogen vibration. (c) The relative Raman peak intensity of nitrogen (blue circles) and oxygen (red squares) as a function of probe intensity. Dotted lines show linear regressions of the respective data points. (d) Cross-correlation of pump and probe pulses (nonresonant background) showing a sinc-squared probe temporal profile with a full-width at half-maximum duration of 0.66 ps.

The entrained vapor was then transported to the interaction region consisting of a two-inch long hollow metal tee having a 5-mm diameter. After passing through the interaction region, the sample was removed via low vacuum exhaust to maintain a steady flow of analyte through the interaction region.

RESULTS

The Raman spectra of air and hydrogen are shown in Figure 2. The spectra are virtually background-free due to the noncollinear geometry employed in the experiment, as well as the cross-polarization of the pump and probe pulses. While it was impractical to vary the pump intensity in the overlap region (as this would change the filament pulse characteristics) we measured the Raman intensities of nitrogen and oxygen as a function of probe energy. For an impulsively excited medium, the signal should vary linearly with probe energy in the low-intensity regime. At higher probe intensities, we expect that stimulated Raman scattering would result in nonlinear Raman gain as a function of probe pulse energy. The stimulated Raman process is seeded by the Stokes/anti-Stokes photons arising from the interference between the probe beam and the impulsively created coherence. Figure 2c shows a linear increase in signal intensity with probe energy, demonstrating that our measurements are made in the low-intensity regime and that the Raman signals can be treated as resulting purely from impulsive excitation. To gain further insight into the generation of the observed Raman spectrum, we also show the filament-probe cross-correlation in Figure 2d. The filament pulse duration can be considered to be much shorter than the probe duration ($\tau_{fil} < \tau_{laser}$ (~50 fs) $\ll \tau_{probe}$ (~1 ps)), so the cross-correlation is taken to be a good approximation of the probe pulse temporal profile. As expected from the method of filtering (a hard-edged slit in a zero-dispersion 4-f compressor), the probe pulse has a Bartlett (sinc-squared) temporal profile. The full-width at half-maximum pulse duration of 660 fs is close to the expected pulse duration for the spectral bandwidth.

To avoid loss of signal due to the frequency-spread dephasing[24] arising from destructive interference at longer time delay between the multitude of rovibrational levels excited, the probe pulse should be as close in time as possible to the impulsive pump pulse. Dephasing can occur rapidly (~3−4 ps for oxygen and nitrogen in air, respectively)[22] and happens on different time scales for different vibrational modes. As a result, measuring at long delay times will lead to variation in the relative peak intensities for modes with different dephasing rates, as well as a decrease in the total signal intensity. An additional consideration that must be made is that temporal overlap between the pump and probe pulses leads to

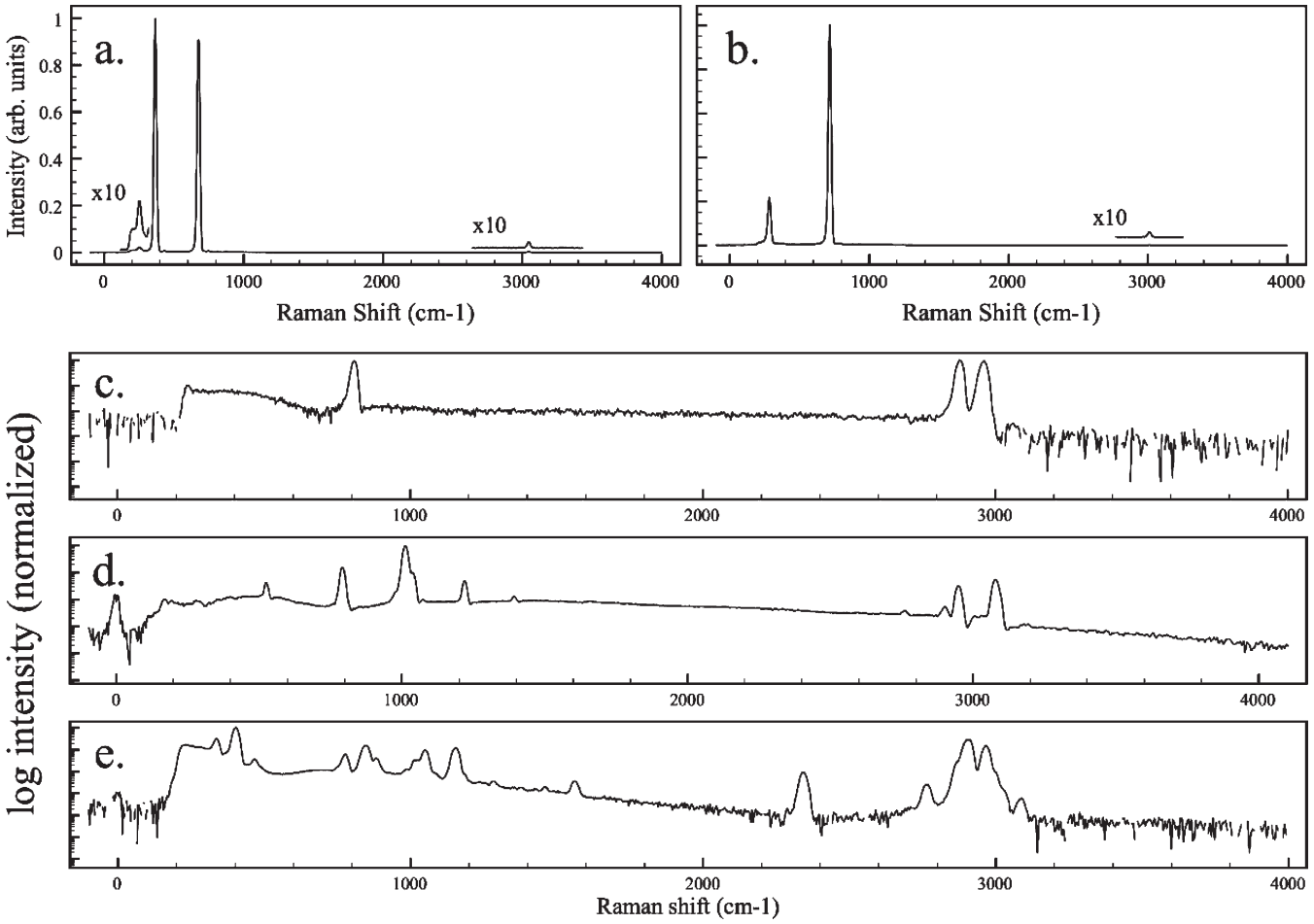

Figure 3. Raman spectra of (a) chloroform, (b) methylene chloride, (c) cyclohexane, (d) toluene, and (e) pentane measured using filament-assisted impulsive Raman spectroscopy (c−e are plotted in logarithmic scale). The lines in (e) at ∼1556 cm^{-1} and ∼2331 cm^{-1} are from oxygen and nitrogen due to incomplete saturation of the detection region with argon and the pentane vapor. Nonresonant background due to cross-phase modulation of the filament and probe pulses results in the slow modulations in the baseline of the spectra to varying degrees depending on sample nonlinearity.

cross-phase modulation. Cross-phase modulation can be avoided by delaying the probe pulse to perform truly background-free measurements. In order to balance these needs in our current experimental configuration, we have set the delay between the impulsive pump and the probe to coincide with the minimum between the central peak in the probe temporal profile and the nearest satellite pulse (a result of the Bartlett profile). Since the probe pulse spectrum is not perfectly rectangular, the temporal intensity does not go to zero at the minimum (as it would for an ideal Bartlett profile), resulting in a coherent background that is superimposed on the Raman spectrum. This could be a potential advantage, however, as the cross-phase modulation-induced background can act as a local oscillator and heterodyne the impulsive Raman signal,[25] which can increase the sensitivity. Heterodyning the signal gives rise to dispersive features because of the π phase shift upon transiting the resonant frequency. Thus, the resonant signal adds constructively and then destructively to the positive phase of the nonresonant background. The interference between the resonant and nonresonant radiation is particularly evident in the toluene spectrum shown in Figure 3d, which displays dispersive features. Such heterodyning has been used in a time-resolved CARS experiment in methanol.[5]

The filament-assisted spectroscopy method was evaluated on a number of samples to investigate the impulsive Raman response of a variety of functional groups and over a range of vibrational frequencies. Figure 3 shows the Raman spectra of chloroform, methylene chloride, cyclohexane, toluene, and pentane. Unlike conventional (spontaneous) Raman spectroscopy, impulsive Raman spectroscopy produces a signal that is proportional to the fourth power of the polarizability.[26] This scaling results in spectral intensities proportional to the square of the spontaneous Raman intensities. Additionally, vapor phase molecules represent the isolated species, resulting in line intensities differing from Raman spectra measured in liquid or solid samples. The Raman spectra of chloroform and methylene chloride (Figure 3a and 3b, respectively) illustrate the low background level and high signal-to-noise achievable over the entire spectral range of the measurement. The 252 cm^{-1} mode of chloroform and the 283 cm^{-1} mode of methylene chloride have signal-to-noise ratios of 18 and 156, respectively, making them easily discernible from the cross-phase modulation background in this region. The low intensity of the C−H stretch mode of methylene chloride, observed at 3010 cm^{-1}, is attributed to the insufficient spectral density of the exciting pulse at the frequency of the mode. However, even under such nonideal conditions, the mode is clearly resolved with a signal-to-noise ratio of 7.3, and has sufficient intensity to be used for characterizing the C−H stretch. The filament-driven impulsive Raman spectrum for cyclohexane is shown in Figure 3c. Consistent with previous measurements of

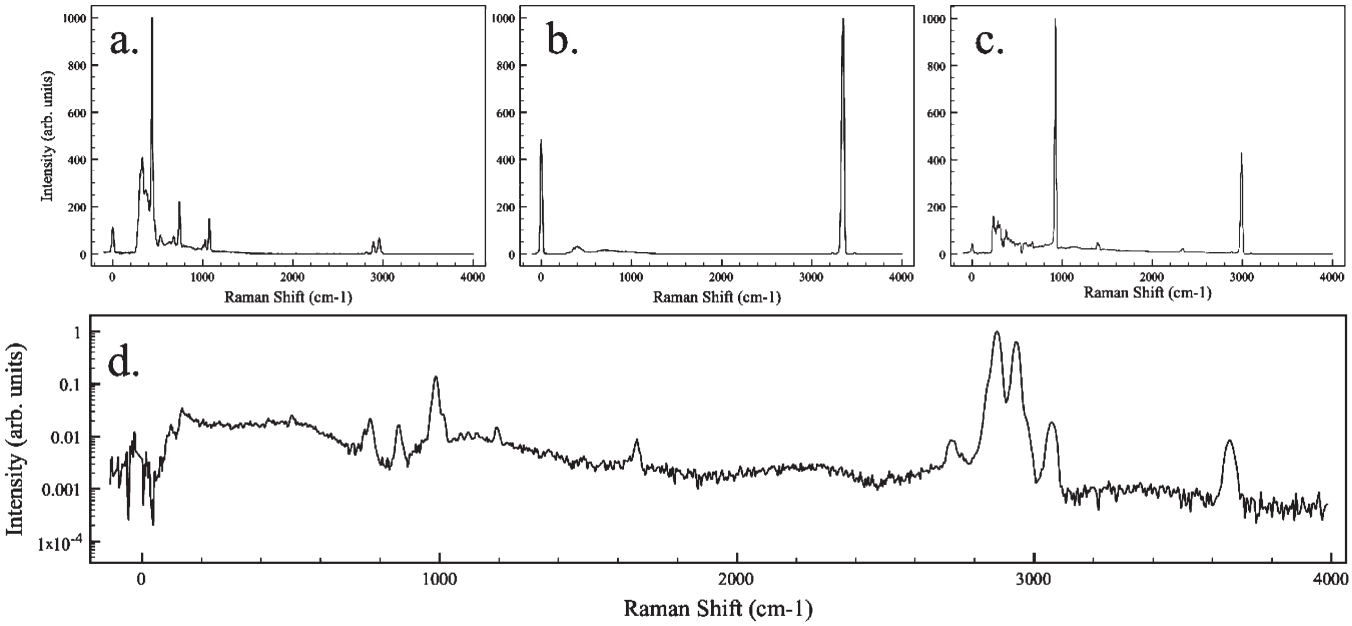

Figure 4. Raman spectra of (a) triethylamine, (b) ammonia gas, (c) nitromethane, and (d) gasoline (log scale) measured using filament-assisted impulsive Raman spectroscopy. The feature at ~3657 cm^{-1} in the gasoline spectrum is water, probably present due to the long exposure of the gasoline to humid air in the laboratory.

the gas phase Raman spectrum,[27] the C−C and C−H stretches have strong signal, while the intermediate peaks are smaller in comparison with the liquid Raman spectrum. The most intense Raman lines at 808, 2878, and 2958 cm^{-1} are clearly observable, while the intermediate modes between 1000 and 1500 cm^{-1} are not observed in the present work due to the fourth-order dependence of the Raman signal on the polarizability. Given the lower intensity Raman response for these modes in the spontaneous Raman spectrum, we expect a quadratic reduction in the impulsive Raman scattering intensity in comparison with the most intense modes observed.

The Raman spectra of toluene and pentane are displayed in Figure 3d,e, respectively. These are representative of a class of molecules commonly found in various fuels. The resolution in the pentane and toluene spectra is sufficient to assign all of the Raman-active molecular modes in the ground state vibrational spectrum and thus enable identification. The Raman peaks from air (oxygen and nitrogen at 1556 and 2331 cm^{-1}, respectively) are visible in the pentane due to incomplete filling of the sample region with the organic vapor and the inert carrier gas (argon). The spectra shown in Figure 3c−e are plotted logarithmically to accommodate the dynamic range of the signal intensities measured. This also clearly shows the contribution of the cross-phase modulation background due to overlap between the pump and the wings of the probe pulse. This effect is small under present experimental conditions, but could in principle be used to advantage in detecting very low intensity modes by decreasing the pump−probe delay, at the expense of convenient determination of line positions in the longer delay configuration.

We investigated several nitrogen-containing organic/inorganic vapors and a commercial fuel mixture in order to evaluate filament-induced impulsive Raman scattering as a means to detect potential signatures for explosive materials. The Raman spectra of ammonia, triethylamine, nitromethane, and gasoline are shown in Figure 4. We observe from our data that organic compounds at high concentrations (saturated or near-saturated vapors), particularly those shown in Figure 4 parts a, c, and d, induce strong cross-phase modulation in the probe beam spectrum (note the intense, modulated background between 0 and 1500 cm^{-1} in Figure 4, parts a, c, and d) due to the increased number of electrons that are easily polarized in these compounds. However, even at the maximum vapor concentrations achievable here, the Raman transitions are still clearly resolved, as is apparent from the observed spectra. These results show promise for application of our technique to remote detection of such signatures.

A limiting factor in this technique is instability in the filament induced by turbulent flow in the measurement region. To avoid this effect, the flow rate of sample was limited to maintain stable filamentation conditions throughout the sample region. Since each sample had both a specific vapor pressure and refractive index contribution (linear and nonlinear), the effect of each sample on the spatial variations in the refractive index in the sample cell differed in magnitude. Thus the maximum tolerable flow rate of sample vapor (entrained in argon) in the detection region was sample specific. Above the maximum tolerable flow rate, the filament became unstable in the detection region, leading to degradation of the signal stability. In addition to the linear effects introduced by turbulence, any spatially inhomogeneous nonlinearity introduced in the pump pulse path by concentrated organic vapors can interrupt the nonlinear filamentation process, leading to the break-up of the filament into multiple filaments.

■ CONCLUSIONS

The method of filamentation-assisted impulsive Raman spectroscopy has been demonstrated for the detection of organic vapor samples in air generated at a distance of ~2.5 m from the laser source. We report the Raman spectra for chloroform, methylene chloride, cyclohexane, toluene, pentane, triethylamine, ammonia,

nitromethane, and gasoline. The latter three compounds represent signatures for explosive materials and suggest applications in remote sensing. Extension of the technique to longer filament generation and detection distances is straightforward and offers a potentially sensitive molecular probe for stand-off detection of gas phase molecules.

AUTHOR INFORMATION

Corresponding Author
*E-mail: rjlevis@temple.edu.

ACKNOWLEDGMENT

This research was funded by the Office of Naval Research Grant No. N00014-10-0293.

REFERENCES

(1) Oron, D.; Dudovich, N.; Silberberg, Y. *Phys. Rev. Lett.* **2002**, *89*, 273001.
(2) Lee, Y. J.; Cicerone, M. T. *Appl. Phys. Lett.* **2008**, *92*, 041108.
(3) Peng, J. H.; Pestov, D.; Scully, M. O.; Sokolov, A. V. *J. Raman Spectrosc.* **2009**, *40*, 795.
(4) Selm, R.; Winterhalder, M.; Zumbusch, A.; Krauss, G.; Hanke, T.; Sell, A.; Leitenstorfer, A. *Opt. Lett.* **2010**, *35*, 3282.
(5) Wang, X.; Wang, K.; Welch, G. R.; Sokolov, A. V. *Phys. Rev. A* **2011**, *84*, 021801.
(6) Katz, O.; Natan, A.; Silberberg, Y.; Rosenwaks, S. *Appl. Phys. Lett.* **2008**, *92*, 171116.
(7) Portnov, A.; Rosenwaks, S.; Bar, I. *Appl. Phys. Lett.* **2008**, *93*, 041115.
(8) Li, H. W.; Harris, D. A.; Xu, B.; Wrzesinski, P. J.; Lozovoy, V. V.; Dantus, M. *Appl. Opt.* **2009**, *48*, B17.
(9) Bremer, M. T.; Wrzesinski, P. J.; Butcher, N.; Lozovoy, V. V.; Dantus, M. *Appl. Phys. Lett.* **2011**, *99*, 101109.
(10) Dhar, L.; Rogers, J. A.; Nelson, K. A. *Chem. Rev.* **1994**, *94*, 157.
(11) Bartels, R. A.; Backus, S.; Murnane, M. M.; Kapteyn, H. C. *Chem. Phys. Lett.* **2003**, *374*, 326.
(12) Marburger, J. H. Self-focusing: Theory (Reprinted from vol 4, pg 35−110, 1975). In *Self-Focusing: Past and Present - Fundamentals and Prospects*; Boyd, R. W., Lukishova, S. G., Shen, Y. R., Eds.; Springer: New York, 2009; Vol. 114; pp 25.
(13) Lange, H. R.; Chiron, A.; Ripoche, J. F.; Mysyrowicz, A.; Breger, P.; Agostini, P. *Phys. Rev. Lett.* **1998**, *81*, 1611.
(14) Mlejnek, M.; Wright, E. M.; Moloney, J. V. *Opt. Lett.* **1998**, *23*, 382.
(15) Braun, A.; Korn, G.; Liu, X.; Du, D.; Squier, J.; Mourou, G. *Opt. Lett.* **1995**, *20*, 73.
(16) Couairon, A.; Mysyrowicz, A. *Phys. Rep.* **2007**, *441*, 47.
(17) Berge, L.; Skupin, S.; Nuter, R.; Kasparian, J.; Wolf, J. P. *Rep. Prog. Phys.* **2007**, *70*, 1633.
(18) Hauri, C. P.; Kornelis, W.; Helbing, F. W.; Heinrich, A.; Couairon, A.; Mysyrowicz, A.; Biegert, J.; Keller, U. *Appl. Phys. B: Laser Opt.* **2004**, *79*, 673.
(19) Stibenz, G.; Zhavoronkov, N.; Steinmeyer, G. *Opt. Lett.* **2006**, *31*, 274.
(20) Calegari, F.; Vozzi, C.; De Silvestri, S.; Stagira, S. *Opt. Lett.* **2008**, *33*, 2922.
(21) Calegari, F.; Vozzi, C.; Negro, M.; De Silvestri, S.; Stagira, S. *J. Mod. Opt.* **2010**, *57*, 967.
(22) Odhner, J. H.; Romanov, D. A.; Levis, R. J. *Phys. Rev. Lett.* **2009**, *103*, 075005.
(23) Odhner, J. H.; Romanov, D. A.; Levis, R. J. *Phys. Rev. Lett.* **2010**, *105*, 125001.
(24) Lucht, R. P.; Roy, S.; Meyer, T. R.; Gord, J. R. *Appl. Phys. Lett.* **2006**, *89*, 251112.
(25) Chang, Y. J.; Cong, P.; Simon, J. D. *J. Phys. Chem.* **1995**, *99*, 7857.
(26) Yan, Y. X.; Nelson, K. A. *J. Chem. Phys.* **1987**, *87*, 6240.
(27) Lorenzo, C. F.; Alcantara, R.; Martin, J. *J. Raman Spectrosc.* **1989**, *20*, 291.